ELSEVIER

Chemical Engineering Science 60 (2005) 5962–5970

Chemical Engineering Science

www.elsevier.com/locate/ces

Exploiting the Bjerknes force in bubble column reactors

Juerg Ellenberger, Jasper M. van Baten, Rajamani Krishna*

Van't Hoff Institute for Molecular Sciences, University of Amsterdam, Nieuwe Achtergracht 166, 1018 WV Amsterdam, The Netherlands

Received 23 October 2004; received in revised form 18 December 2004; accepted 4 March 2005
Available online 17 May 2005

Abstract

A bubble column, subjected to low-frequency vibrations, displays maxima in the gas holdup when operated at certain frequencies. These maxima represent various harmonics created by standing waves. The axial distribution of gas holdup was measured for these harmonics to demonstrate that the gas holdup at the anti-nodes is higher than at the nodes; this phenomena is a manifestation of the primary Bjerknes force acting on the bubbles. The Bjerknes force can be exploited to obtain the optimum increase in the gas holdup for a given set of operating conditions.

Keywords: Harmonics; Sound waves; Bubble columns; Anti-nodes; Nodes; Gas holdup

1. Introduction

A bubble column reactor is commonly used in the process industries for carrying out a variety of liquid phase reactions (Deckwer, 1992). In many applications, especially for mass transfer limited reactions, it is necessary to have a precise control on the bubble sizes for improved conversion and selectivity. Our earlier work has shown that the application of low-frequency vibrations in the 20–100 Hz range can significantly improve the gas holdup ε and volumetric mass transfer coefficient $k_L a$ (Ellenberger and Krishna, 2002, 2003; Krishna and Ellenberger, 2002). For a specified set of operating conditions (dispersion height H and superficial gas velocity U), the improvement in the gas holdup ε was found to be a non-monotonous function of the vibration frequency f (Krishna and Ellenberger, 2002), displaying maxima at a set of frequencies suggesting that the bubble column was operating at different harmonics. However, the harmonic operation of the bubble column was not investigated in detail and neither was the theoretical background explored to any extent.

The theoretical background on the influence of sound waves on single gas bubbles is well documented in the literature (Brennen, 1995; Leighton, 1994; Leighton et al., 1990). When a gas bubble in liquid is subjected to an acoustic pressure field, it can undergo volume pulsations. If the acoustic pressure gradient is non-zero, then it can couple with the bubble oscillations to produce a translation force on the bubble. This is the primary Bjerknes force (Bjerknes, 1909). Consider a bubble of volume $V = \frac{4}{3}\pi r^3$ subject to an oscillating pressure field given by $P(z,t) = A_p \sin(2\pi f t)\sin(2\pi\lambda z/H)$ where f is the vibration frequency and λ is the wave length of the sine wave. The pressure profiles are illustrated in Fig. 1a for five different harmonics, HM-1, 2, 3, 4 and 5 corresponding to wave lengths $\lambda = 4H, 4H/3, 4H/5, 4H/7$ and $4H/9$. The Bjerknes force acting on the bubble due to volume oscillations is given by the time average of

$$-V(t)\frac{\mathrm{d}P(z,t)}{\mathrm{d}z}, \quad \text{i.e.}$$

$$F_{\text{vib}} = -\left\langle \frac{4}{3}\pi r(t)^3 A_p \frac{2\pi\lambda}{H} \sin(2\pi f t)\cos\left(2\pi\lambda\frac{z}{H}\right)\right\rangle,$$

where the braces represent time-averaging. .

* Corresponding author. Tel.: +31 20 525 7007; fax: +31 20 525 5604.
E-mail address: R.Krishna@uva.nl (R. Krishna).

0009-2509/$ - see front matter
doi:10.1016/j.ces.2005.03.036

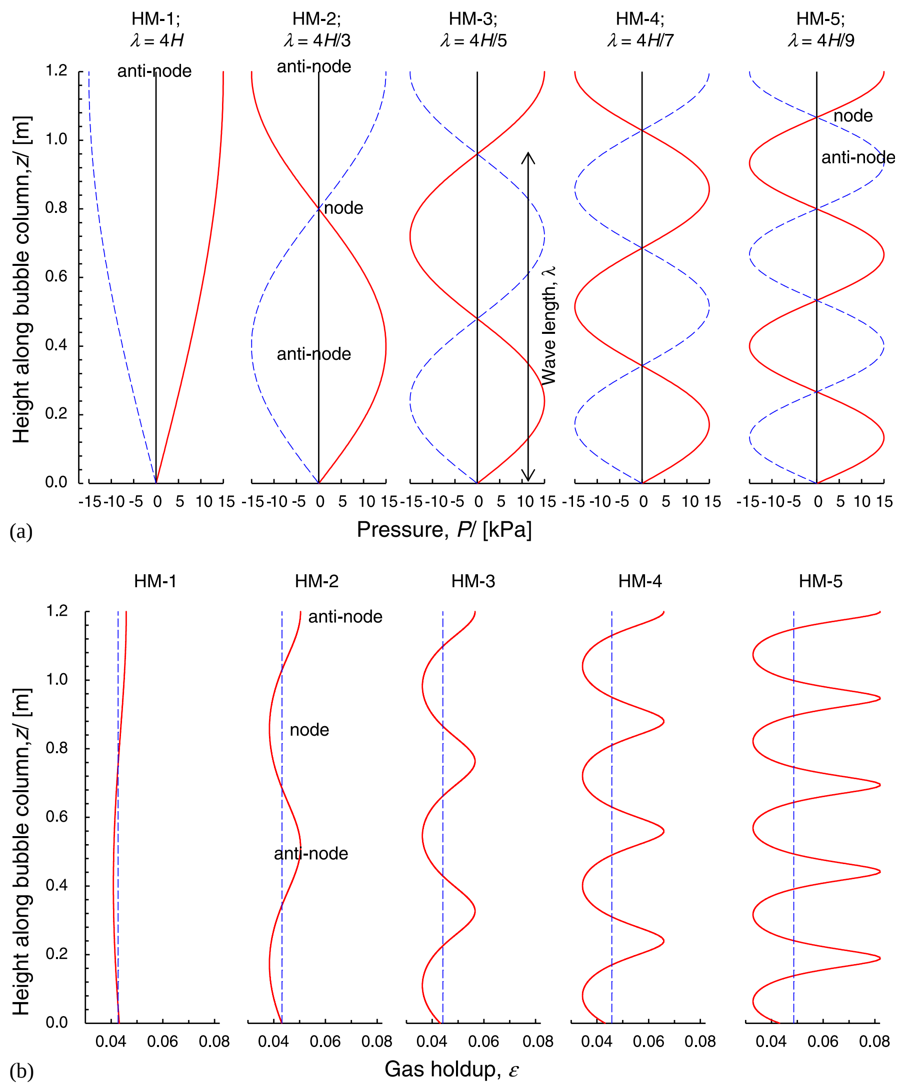

Fig. 1. Harmonics in bubble column operation showing (a) pressure oscillations, and (b) gas holdup as a function of column height. The calculations are carried out using the following set of parameters: $H = 1.2\,\mathrm{m}$, $U = 0.01\,\mathrm{m\,s^{-1}}$, vibration frequency $f = 75\,\mathrm{Hz}$; ambient pressure $P_0 = 100\,\mathrm{kPa}$, pressure amplitude $A_p = 15\,\mathrm{kPa}$, bubble radius $r_0 = 2.5\,\mathrm{mm}$, surface tension $\sigma = 0.073\,\mathrm{N\,m^{-1}}$, $C_D = 1.21$.

The variation of the bubble radius with time is described by the Rayleigh–Plesset (R–P) equation (Brennen, 1995; Leighton, 1994; Leighton et al., 1990):

$$\frac{\partial^2 r}{\partial t^2} = -\frac{3}{2r}\frac{\partial r}{\partial t} + \left(\left(P_0 + 2\frac{\sigma}{r_0}\right)\left(\frac{r_0}{r}\right)^3 - 2\left(\frac{\sigma}{r}\right) - 4\frac{\mu}{r}\frac{\partial r}{\partial t} - P_0 - P(z,t)\right).$$

Let us apply this theory to describe the influence of vibrations in an air–water bubble column with a dispersion height of 1.2 m subject to vibrations at the bottom at 75 Hz with a pressure amplitude $A_p = 15\,\mathrm{kPa}$. Let us assume that the bubble radius $r_0 = 2.5\,\mathrm{mm}$, with a drag coefficient $C_D = 1.21$; these values are typical for air–water bubble columns operating in the homogeneous bubbly flow regime (Clift et al., 1978; Krishna et al., 1999). The use of the empirical drag coefficient should ensure that the results can be used also for practical cases where the bubbles are not spherical. When the bubble column is subject to vibrations at the bottom the bubble velocity is governed by the sum of the Bjerknes, buoyancy and drag forces:

$$\frac{\partial u}{\partial t} = \frac{\partial^2 z}{\partial t^2} = -V\frac{\mathrm{d}P(z,t)}{\mathrm{d}z} + (\rho_L - \rho_G)Vg - \frac{1}{2}C_D\rho_L|u|u\pi r^2.$$

Solution of this equation along with the R–P equation allows calculation of the local rise velocity, and the gas holdup, along the column height for a bubble column operating at $U = 0.01\,\mathrm{m\,s^{-1}}$. The calculations for the local gas holdup are presented in Fig. 1b for the five different harmonics. We note that in the standing-wave field bubbles tend to collect in

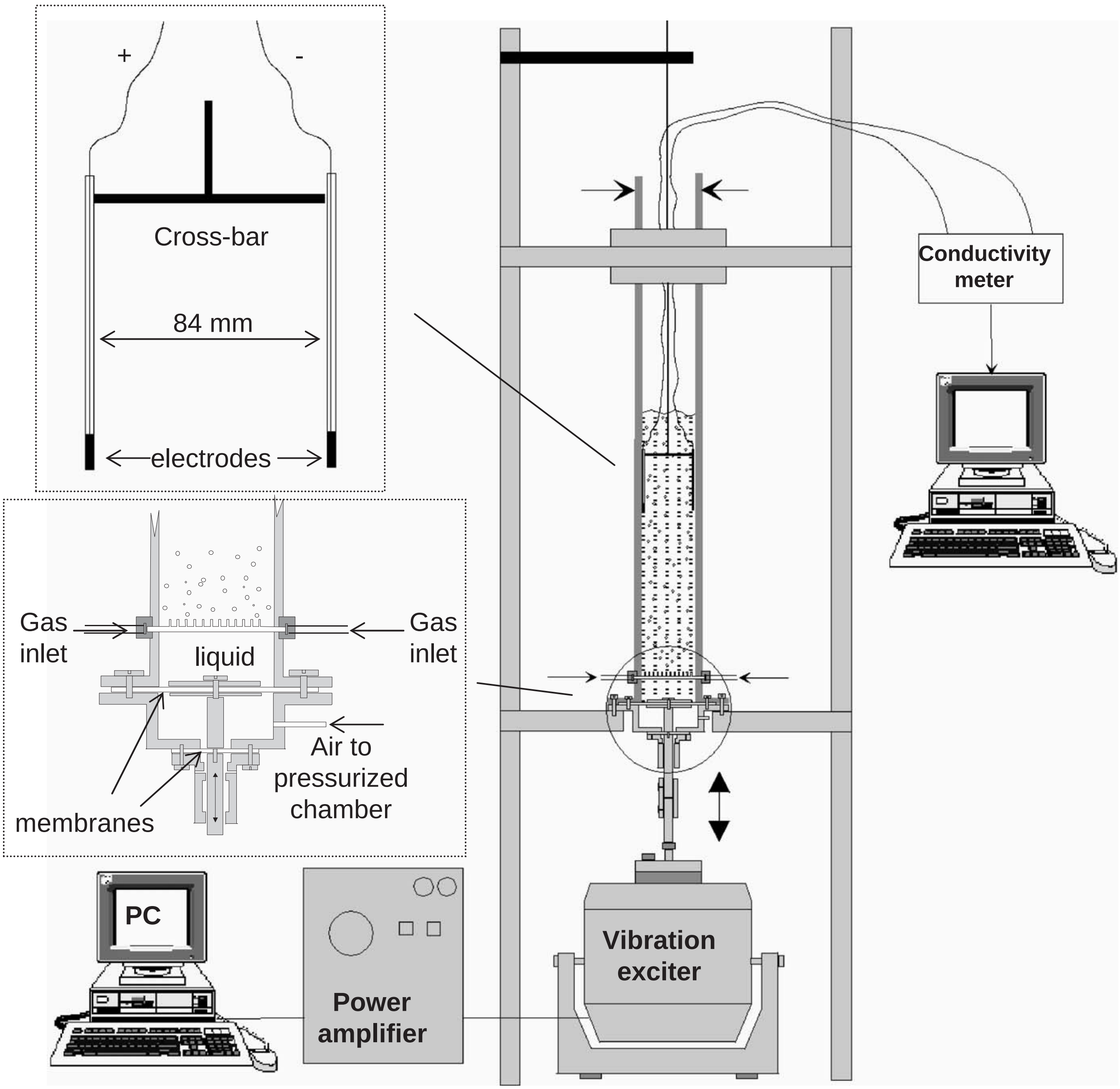

Fig. 2. Experimental set up of vibrationally excited bubble column. The two insets on the left side the figure show the details of the 12-capillary gas distribution device and the movable two-electrode system for determination of the axial gas holdup distribution. Further details of the experimental setup are available elsewhere (Ellenberger and Krishna, 2004).

higher concentration at the pressure anti-nodes (Leighton et al., 1990). The dashed lines in Fig. 1b represent the height-averaged gas holdup; this average holdup increases when the column is operated at the higher harmonics.

The major objective of the present communication is to investigate the bubble column operation at the various harmonics in more detail and to verify the above predictions that the Bjerknes force results in higher gas holdups at the pressure anti-nodes. Such a result has never been demonstrated before in the published literature. Our study will help to optimize the operating conditions to be chosen so as to obtain the maximum improvement in gas holdup in a vibrationally excited bubble column.

2. Experimental set-up and procedures

The experimental set-up consists of a bubble column, a vibration exciter, a power amplifier, a vibration controller and a personal computer. A schematic diagram of the experimental set-up is given in Fig. 2 The bubble column, made of polyacrylate, has an inner diameter of 0.10 m and a height of 2.0 m. The bottom of the column is sealed by a silicon rubber membrane of 0.4 mm thickness and clamped between two metal disks of 0.096 m in diameter (see inset to Fig. 2). At a distance of 0.12 m above the membrane, air is fed to the bubble column through 12 stainless steel capillaries of 0.9 mm i.d. The gas flow is controlled by means of a calibrated flowmeter (Brooks). In order to hold the membrane at constant vertical position after filling the column with the liquid phase, a chamber for pressure compensation is mounted below the membrane. The membrane is connected to an air-cooled vibration-exciter (TIRAvib 5220, Germany). The amplifier of this vibration-exciter is controlled by the *SignalCalc* 550 *Vibration-controller* in a PC environment. The frequency range is 10–5000 Hz. Depending on the frequency the amplitude can be varied between 0 and 25 mm. Further details of the experimental set-up including photographs of the rig are available elsewhere (Ellenberger and Krishna, 2004). All the measurements have been carried out at room temperature with air as the gas phase and demineralized water as the liquid phase. The pressure at the top of the column is atmospheric. All experiments reported here have been carried out with the liquid in batch mode.

The local gas holdup as function of the vertical position in the column is measured by means of a conductivity sensor, shown in the top left inset to Fig. 2. The two stainless steel electrodes ($5 \times 5 \times 20\,\mathrm{mm}^3$) of the conductivity sensor were fixed at the bottom of two 6 mm o.d. glass tubes. The glass tubes with a length 0.14 m are connected to a crossbar of 6 mm diameter at the top of the tubes in order to keep the distance between the electrodes constant. The conductivity sensor is fixed on a 1.5 m glass rod with a diameter of 6 mm to position the sensor in the bubble column at a chosen axial position. The two electrodes are connected to a Consort K920 portable conductivity meter. The bubble column is filled with dimineralized water containing 0.03% v/v NaCl. When the operation of the vibrated bubble column is stabilized, the output signal of the conductivity meter is stored on a PC during 3 min with a sample rate of 10 Hz. During the last minute of the sampling time the gas flow and the vibration exciter are turned off in order to obtain a reference signal corresponding to a gas holdup value of zero. A typical example of the output signal is given in Fig. 3. The average value of the output signal, ϕ_U, during operation at superficial gas velocity U is calculated in the time interval between 0 and 110 s and the average value at no-gas condition $\phi_{U=0}$ is calculated in the time interval 150–180 s. Assuming a linear relationship between output signal and gas holdup ε_G with the boundary values, the local cross sectional gas holdup is calculated from

$$\varepsilon = 1 - \frac{\phi_U}{\phi_{U=0}}. \tag{1}$$

For the conditions shown in Fig. 3, for example, the calculated gas holdup at the chosen height along the column is equal to $\varepsilon = 1 - 0.1758/0.2102 = 0.1635$.

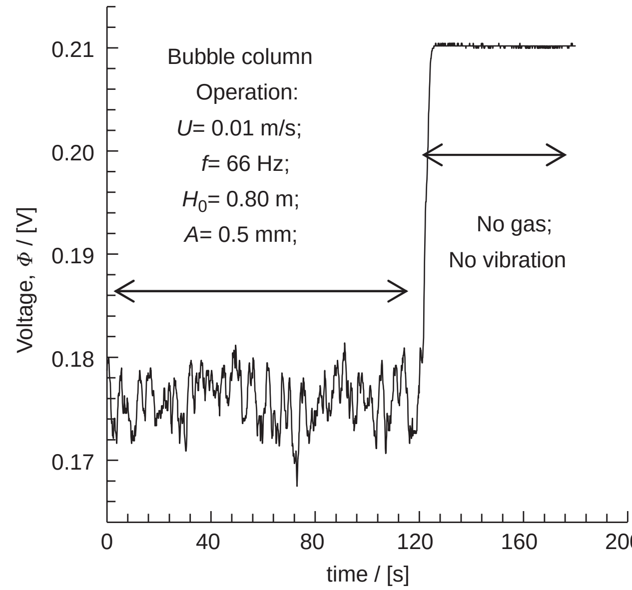

Fig. 3. Typical output of conductivity sensor, measured at a height $H = 0.25\,\mathrm{m}$ above the vibration piston. The measurement is recorded for 120 s during bubble column operation ($U = 0.01\,\mathrm{m\,s^{-1}}$; $f = 66\,\mathrm{Hz}$; $H_0 = 0.80\,\mathrm{m}$; $A = 0.5\,\mathrm{mm}$) and the gas is switched off at $t = 120\,\mathrm{s}$.

Additionally the overall gas holdup was determined by visually recording the dispersion height H; the gas holdup is then calculated from

$$\langle \varepsilon \rangle = 1 - \frac{H_0}{H}, \tag{2}$$

where H_0 is the height of pure liquid above the gas distributor, when no gas is injected into the system.

For each measurement campaign, video recordings of the column operation at the various positions along the column height were made using a Photron Fastcam-ultima 40 K high-speed (max 4500 fps) video camera. These video recordings can be viewed on our web site (Ellenberger and Krishna, 2004). Snapshots from these video recordings are exemplified in Fig. 4a–c for operation at $U = 0.0041\,\mathrm{m\,s^{-1}}$ and $H_0 = 1.1\,\mathrm{m}$. Fig. 4a shows the snapshot of a bubble column not subjected to vibrations. Fig. 4b and c show snapshots taken at the node and anti-node, respectively, of the same column subject to vibrations $f = 95\,\mathrm{Hz}$, $A = 0.3\,\mathrm{mm}$ operating at the third harmonic, HM-3. The snapshots demonstrate the dramatic increase in the gas holdup due to vibrations, and also the significantly higher concentration of bubbles at the anti-nodes as compared to that at the nodes. An important observation from these snapshots is that the bubble sizes at both the nodes (Fig. 4b) and anti-nodes (Fig. 4c) are significantly smaller than for the case without vibration (Fig. 4a). Also, the bubble concentrations at both the nodes and anti-nodes are higher than for the no-vibrations case.

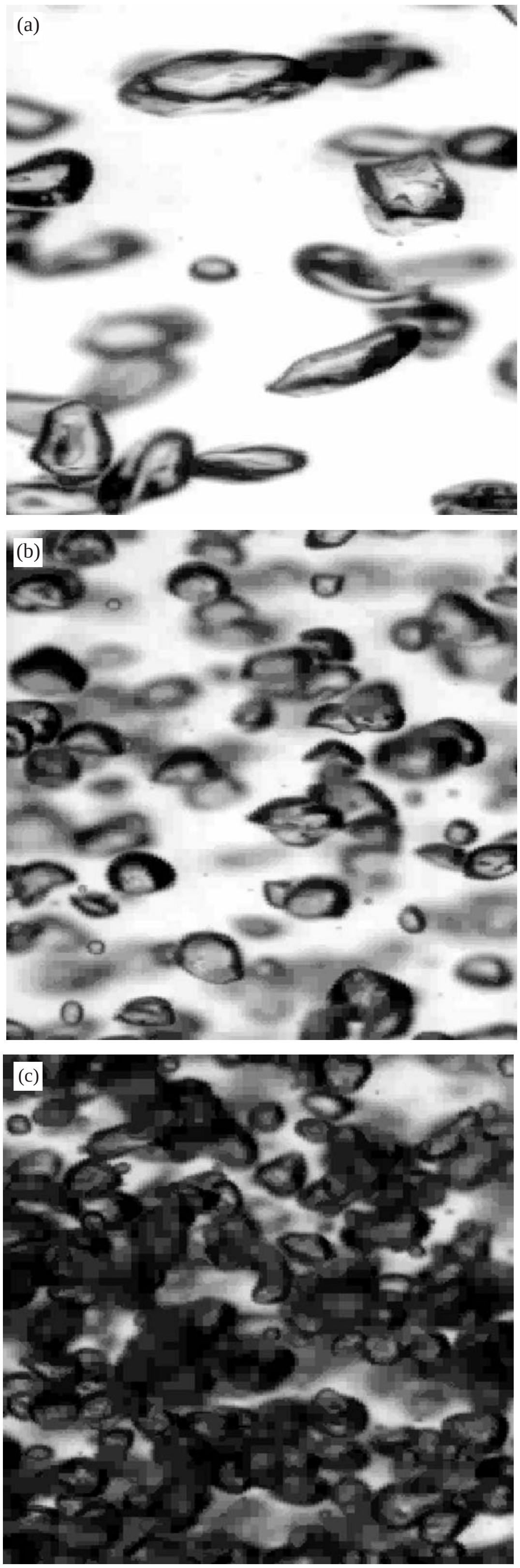

Fig. 4. Close-up snapshots of the column operation at $U = 0.0041\,\mathrm{m\,s^{-1}}$, $H_0 = 1.1\,\mathrm{m}$: (a) without vibrations, and (b,c) with vibrations at $f = 95\,\mathrm{Hz}$ and $A = 0.3\,\mathrm{mm}$ operating at the third harmonic HM-3 at (b) node and (c) anti-node.

3. Experimental results and discussion

Consider first operation at $U = 0.01\,\mathrm{m\,s^{-1}}$ with a vibration amplitude $A = 0.5\,\mathrm{mm}$ and $H_0 = 0.8\,\mathrm{m}$. The average gas holdup $\langle\varepsilon\rangle$ was determined for a range of frequencies varying from 0 to 80 Hz and the enhancement in the gas holdup with respect to the average gas holdup for the no-vibration case, i.e. $f = 0\,\mathrm{Hz}$, is plotted in Fig. 5a as a function of the vibration frequency f. There are three peaks in the gas holdup, at $f = 20, 44$ and 66 Hz. These three peaks correspond to HM-1, 2 and 3 as illustrated in Fig. 1b. This was also verified by the local gas holdup measurements at these three frequencies (see Fig. 6a–c). The column height is not high enough to realise the fourth and fifth harmonics and frequencies higher than 80 Hz cannot be realized due to intense splashing at the top of the column. To realise the higher harmonics we need to increase the dispersion height; this is demonstrated in the results presented in Fig. 5b for $H_0 = 1.1\,\mathrm{m}$. The column is now too high to realise the first harmonic, but amplitude $A = 0.5\,\mathrm{mm}$ the column is seen to exhibit the second, third and fourth harmonics at 35, 55 and 75 Hz. However, due to intense splashing at frequencies exceeding 80 Hz, the fifth harmonic cannot be realised for $A = 0.5\,\mathrm{mm}$. The fifth harmonic can be realised with a frequency of 94 Hz if the vibration amplitude is reduced to $A = 0.4\,\mathrm{mm}$, as can be seen in Fig. 5b. The local gas holdup measurements verifying the third, fourth and fifth harmonics are shown in Fig. 6d–f.

It should be noted that the average gas holdup for the no-vibrations case is significantly lower than that gas holdup at either the anti-node or node. This can be explained on the basis of the snapshots shown in Fig. 4a–c. which show that the bubble concentrations are significantly lower than at either node or anti-node for a harmonically vibrated column.

Several other measurement campaigns were carried out to determine the column harmonics. For example, Fig. 5c and d show the results of the campaign with $U = 0.0041\,\mathrm{m\,s^{-1}}$, $A = 0.3\,\mathrm{mm}$ wherein H_0 is varied in steps from 0.85 to 1.35 m. Examination of these results show that for low dispersion heights only the first and second harmonics can be realised and for the high dispersion heights only the second and third harmonics can be realised. For intermediate dispersion heights we can realise HM-1, 2 and 3. To emphasise this point further we present the results of a campaign in Fig. 7 of a campaign at $U = 0.0041\,\mathrm{m\,s^{-1}}$, $A = 0.3\,\mathrm{mm}$ wherein the vibration frequency is held constant at $f = 55\,\mathrm{Hz}$ and the total dispersion height is varied in small steps from 1 to 2 m. Two peaks are observed, at $H = 1.18$ and 1.82 m, corresponding respectively, to HM-2 and HM-3, underlining the fact that the higher harmonics are realised at higher dispersion heights.

In Fig. 8 we have plotted the velocity of the resonant waves, $w = \lambda f$ against $\langle\varepsilon\rangle$ for harmonic operation (i.e., corresponding the gas holdup peaks). The resonant wave velocity represents the velocity at which the sound wave travels in the gas liquid dispersion. With increasing gas holdup the

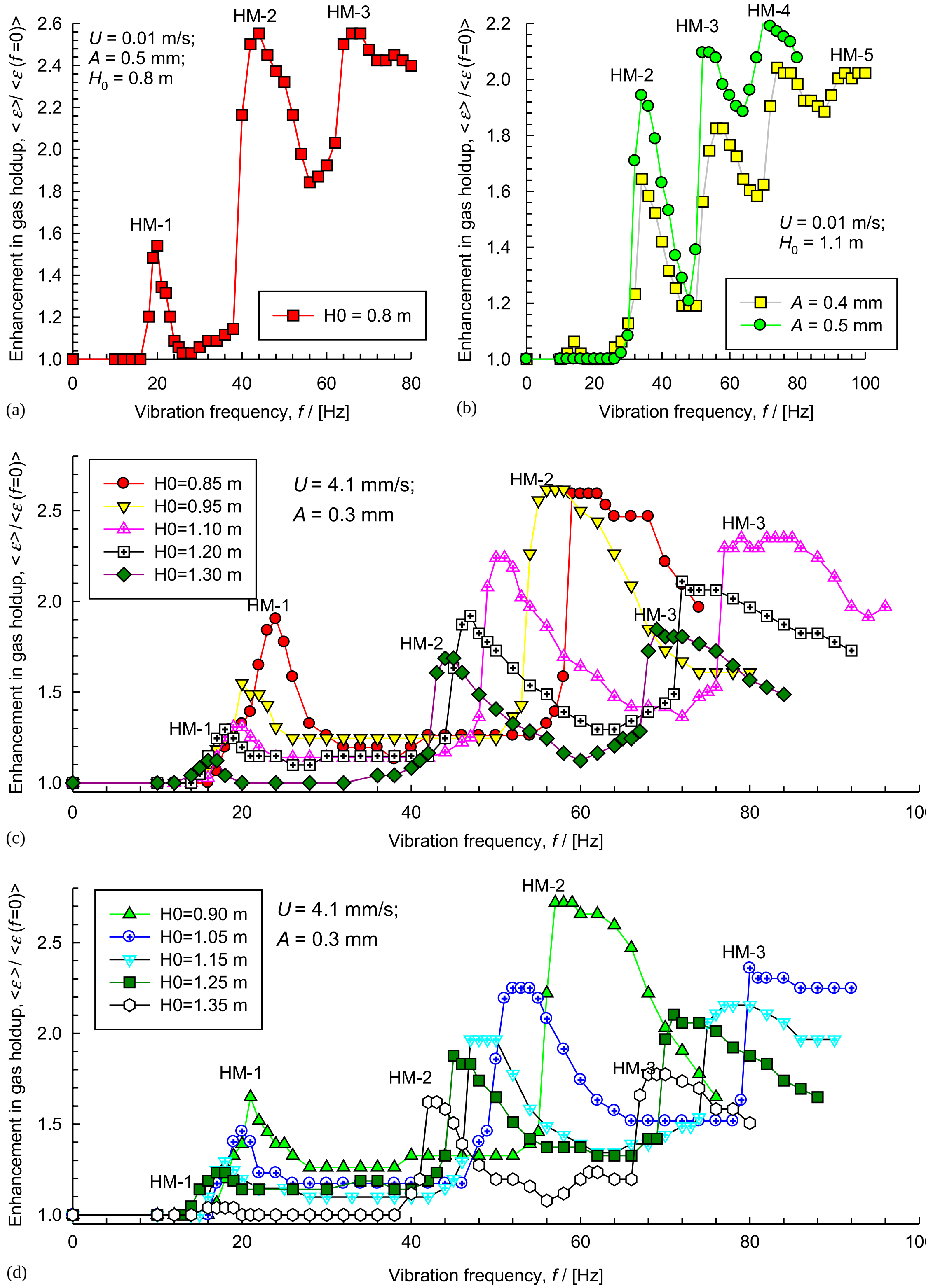

Fig. 5. Gas holdup enhancement as a function of the vibration frequency f for bubble column operating at: (a) $U = 0.01\,\mathrm{m\,s^{-1}}$, $H_0 = 0.80\,\mathrm{m}$, $A = 0.5\,\mathrm{mm}$; (b) $U = 0.01\,\mathrm{m\,s^{-1}}$, $H_0 = 1.1\,\mathrm{m}$, $A = 0.4, 0.5\,\mathrm{mm}$; and (c,d) $U = 0.0041\,\mathrm{m\,s^{-1}}$, $A = 0.3\,\mathrm{mm}$, $H_0 = 0.85$–$1.35\,\mathrm{m}$.

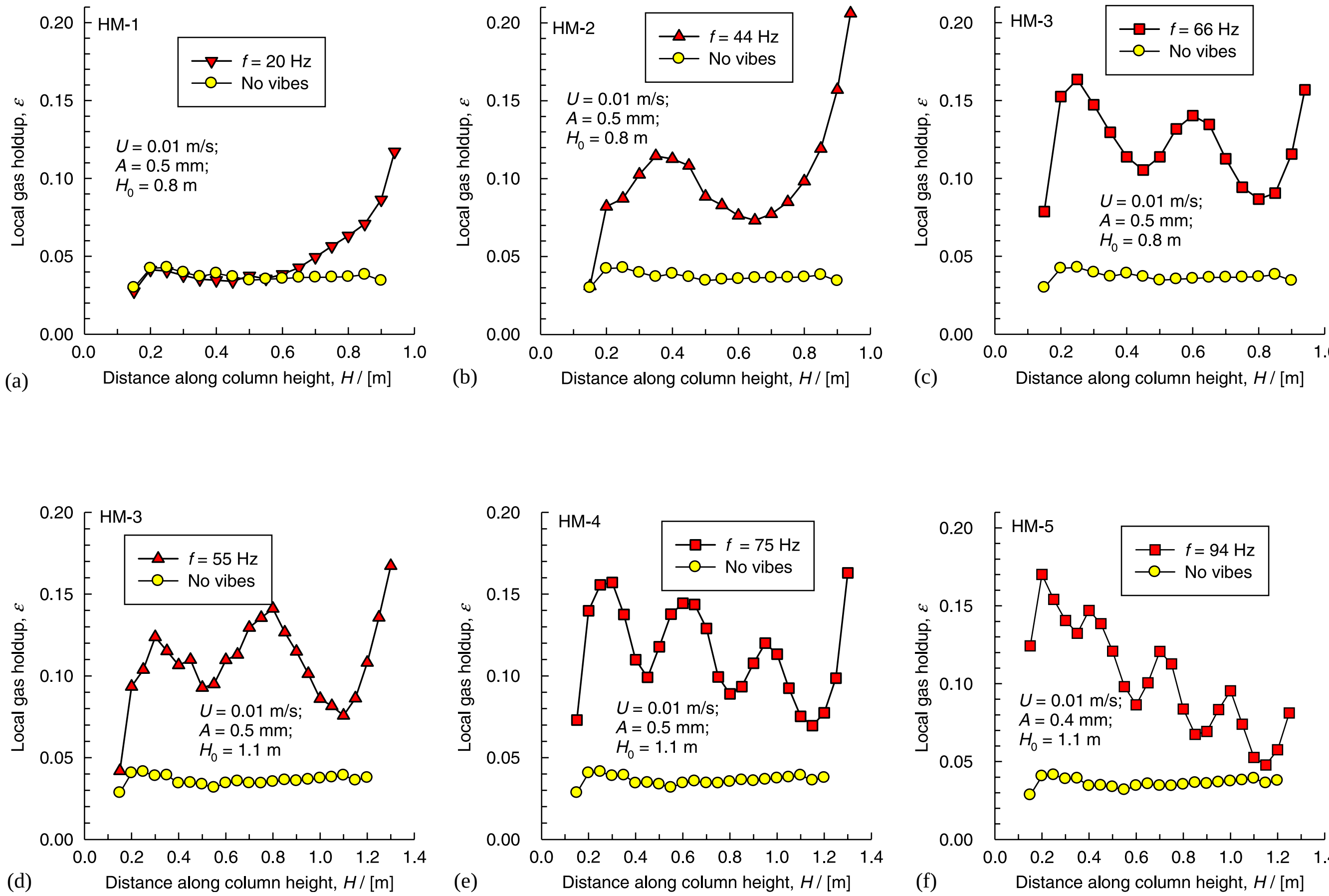

Fig. 6. The local gas holdup along the column as function of height above the vibration piston is shown for (a–c) $U = 0.01\,\mathrm{m\,s^{-1}}$; $H_0 = 0.80\,\mathrm{m}$; $A = 0.5\,\mathrm{mm}$ and (d–f) $U = 0.01\,\mathrm{m\,s^{-1}}$; $H_0 = 1.1\,\mathrm{m}$. High-speed recordings showing close-ups of the nodes and anti-nodes can be viewed on our web site (Ellenberger and Krishna, 2004).

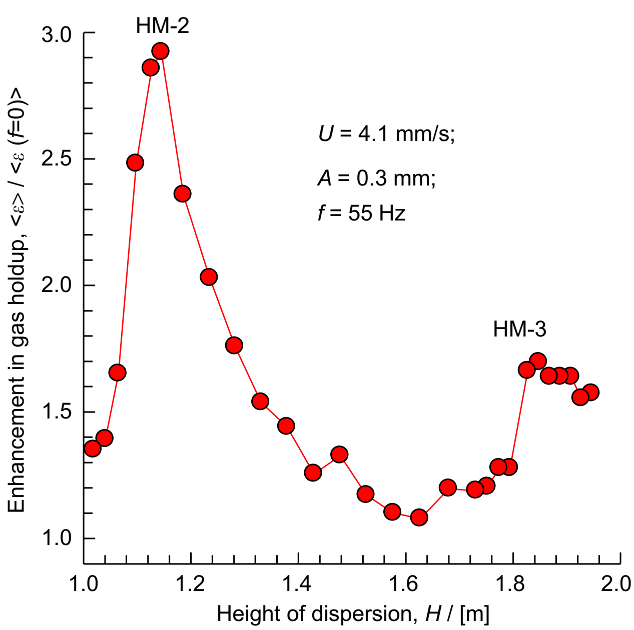

Fig. 7. Gas holdup enhancement as a function of the dispersion height for bubble column operating at $U = 0.0041\,\mathrm{m\,s^{-1}}$; $A = 0.3\,\mathrm{mm}$, $f = 55\,\mathrm{Hz}$.

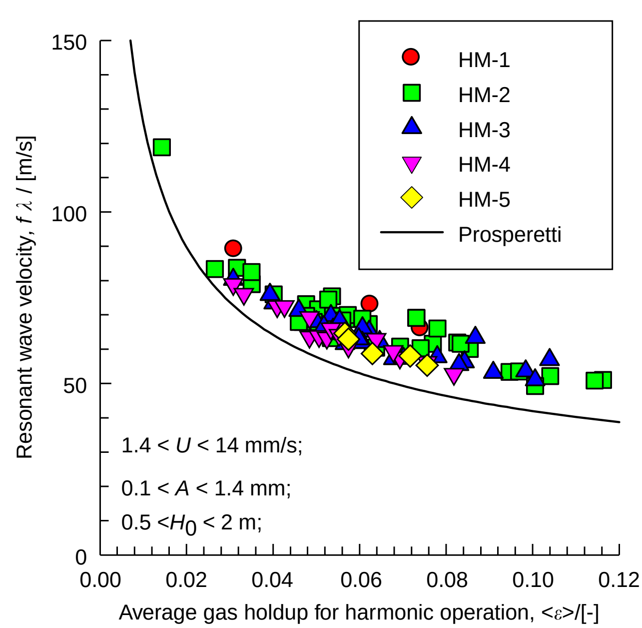

Fig. 8. Resonant wave velocity, $w = \lambda f$, obtained from the experiments at various harmonics compared with the calculations from Eq. (3) derived by Prosperetti (1984).

velocity of sound waves in the dispersion decreases. The continuous solid line in Fig. 8 represents the theoretical expression of Prosperetti (1984) for sound velocity in bubbly dispersions:

$$\frac{1}{w^2} = \frac{\varepsilon}{w_G^2} + \frac{(1-\varepsilon)^2}{w_L^2}\left(1 + \frac{\rho_G}{\rho_L}\frac{\varepsilon}{1-\varepsilon}\right) - (\rho_L - \rho_G)\varepsilon(1-\varepsilon)\frac{1}{V}\frac{\mathrm{d}V}{\mathrm{d}p}, \tag{3}$$

where w_G and w_L represent the velocity of sound in air and water at ambient conditions; these values are taken to be 350 and 1500 $\mathrm{m\,s^{-1}}$, respectively. The agreement is qualitatively very good. Extrapolation of curve to zero-gas holdup yields the sound velocity in water. Since the higher harmonics lead to higher enhancement of gas holdup, the w–$\langle\varepsilon\rangle$ relationship provides a means of tuning the vibration frequency for a given dispersion height in order to achieve harmonic operation.

4. Conclusions

The following major conclusions can be drawn from the work reported in this study:

1. A bubble column subject to vibrations shows maxima in the gas holdup at certain frequencies, corresponding to various harmonics in the column operation. In our experiments the first five harmonics could be detected. The wave lengths corresponding to these harmonics are given by $\lambda = 4H, 4H/3, 4H/5, 4H/7$ and $4H/9$ where H is the dispersion height.
2. Measurements of the local gas holdup along the column height for harmonic operation show a higher bubble concentration at the pressure anti-nodes. These high concentration is the manifestation of the Bjerknes force acting on the bubbles. The gas holdup enhancement due to vibrations is higher for the higher harmonics.
3. The wave velocity $w = \lambda f$ corresponding to these harmonics is found to be a unique function of the average gas holdup in the column. The experimentally obtained value of w is in good qualitative agreement with the expression for the velocity of sound in gas–liquid dispersions derived by Prosperetti (1984). Since the higher harmonics lead to higher enhancement of gas holdup, the w–$\langle\varepsilon\rangle$ relationship provides a means of tuning the vibration frequency for a given dispersion height in order to achieve harmonic operation.
4. There are distinct advantages for operating the vibrated bubble column under the higher harmonic modes, because the average gas holdup would be higher than if the column were not operated harmonically.

The vast potential of exploiting the Bjerknes force to improve the performance of gas–liquid bubble columns is largely untapped and we take a first step in this direction in this work.

Notation

A	vibration amplitude, m
A_p	vibration amplitude expressed in pressure units, Pa
C_D	drag coefficient of bubble, dimensionless
f	vibration frequency, Hz
g	gravitational acceleration, $\mathrm{m\,s^{-2}}$
H	total height of dispersion, m
H_0	clear liquid height above the gas distributor, m
P	pressure, Pa
P_0	ambient pressure, Pa
r	radius of bubble, m
r_0	initial radius of bubble, m
t	time, s
u_0	bubble rise velocity without sound field, $\mathrm{m\,s^{-1}}$
U	superficial gas velocity, $\mathrm{m\,s^{-1}}$
V	bubble volume, $\mathrm{m^3}$
w	resonant wave velocity, $\mathrm{m\,s^{-1}}$
z	distance along the height of bubble column, m

Greek letters

ε	local gas holdup at height z above the distributor, dimensionless
$\langle\varepsilon\rangle$	average gas holdup, dimensionless
λ	wave length, m
μ	liquid viscosity, Pa
ρ_G	gas density, $\mathrm{kg\,m^{-3}}$
ρ_L	liquid density, $\mathrm{kg\,m^{-3}}$
σ	surface tension, $\mathrm{N\,m^{-1}}$
ϕ	voltage, V

Subscripts

G	gas phase
L	liquid phase

Acknowledgements

The authors acknowledge two Grants Programmasubsidie and TOP Subsidy from the Netherlands Foundation for Fundamental Research (CW-NWO) for development of novel concepts in reactive separations.

References

Bjerknes, V., 1909. Die Kraftfelder. F. Vieweg, Braunschweig.

Brennen, C.E., 1995. Cavitation and Bubble Dynamics. Oxford University Press, New York.

Clift, R., Grace, J.R., Weber, M.E., 1978. Bubbles, Drops and Particles. Academic Press, San Diego, CA.

Deckwer, W.D., 1992. Bubble Column Reactors. Wiley, New York, NY.

Ellenberger, J., Krishna, R., 2002. Improving mass transfer in gas–liquid dispersions by vibration excitement. Chemical Engineering Science 57, 4809–4815.

Ellenberger, J., Krishna, R., 2003. Shaken, not stirred, bubble column reactors: enhancement of mass transfer by vibration excitement. Chemical Engineering Science 58, 705–710.

Ellenberger, J., Krishna, R., 2004. Influence of sound waves on the gas holdup in a bubble column, 3 September 2004, http://ct-cr4.chem.uva.nl/GasHoldupSoundWaves/

Krishna, R., Ellenberger, J., 2002. Improving gas–liquid contacting in bubble columns by vibration excitement. International Journal of Multiphase Flow 28, 1223–1234.

Krishna, R., Urseanu, M.I., van Baten, J.M., Ellenberger, J., 1999. Wall effects on the rise of single gas bubbles in liquids. International Communications in Heat and Mass Transfer 26, 781–790.

Leighton, T.G., 1994. The Acoustic Bubble. Academic Press, San Diego.

Leighton, T.G., Walton, A.J., Pickworth, M.J.W., 1990. Primary Bjerknes forces. European Journal of Physics 11, 47–50.

Prosperetti, A., 1984. Bubble phenomena in sound fields: part two. Ultrasonics 22, 115–124.